Applied Energy 330 (2023) 120342

Contents lists available at ScienceDirect

Applied Energy

journal homepage: www.elsevier.com/locate/apenergy

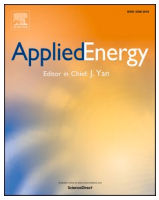

Viability of waste heat capture, storage, and transportation for decentralized flowback and produced water treatment

Brandi M. Grauberger [a], Garrett M. Cole [b], Cristian A. Robbins [c], Jason C. Quinn [b], Tiezheng Tong [c,*], Todd M. Bandhauer [a,*]

[a] REACH Co-Lab, Department of Mechanical Engineering, Colorado State University, Fort Collins, CO 80523, United States
[b] Department of Mechanical Engineering, Colorado State University, Fort Collins, CO 80523, United States
[c] Department of Civil and Environmental Engineering, Colorado State University, Fort Collins, CO 80523, United States

HIGHLIGHTS

- Thermodynamic modelling of waste heat storage and utilization.
- Modelling of changing operating parameters for thermally driven desalination.
- Comparisons of materials for low temperature waste heat storage.
- Development of apparent specific energy consumption.

ARTICLE INFO

Keywords:
Waste heat utilization
Energy storage materials
Membrane distillation
Flowback and produced water treatment
Thermodynamic modelling

ABSTRACT

The use of waste heat has been proposed to reduce the energy footprint of membrane distillation for flowback and produced water (FPW) treatment. However, its feasibility has not been fully understood for FPW treatment. Accordingly, this study performs systematic assessments through thermodynamic modelling of waste heat capture, storage, and transportation for decentralized FPW treatment at well pads located in the Denver-Julesburg Basin. A wide range of sensible, phase-change, and thermo-chemical storage materials were assessed for their effectiveness at the utilization of waste heat from on-site hydraulic fracturing engines and natural gas compressor stations, in order to overcome the temporal or spatial mismatch between waste heat availability and FPW generation. Our results show that the type of storage material being used can have a high impact on the efficiency of waste heat utilization and the treatment capacity of membrane distillation. Sensible storage materials only utilize sensible heat capacities, while phase-change materials have improved performance because they are able to additionally store latent heat. However, sensible and phase-change storage materials lose 11–83% of heat due to conversion inefficiencies caused by their changing temperatures. Thermo-chemical materials, on the other hand, have the highest potential for use because they collect and release heat at constant temperatures. We identified three thermo-chemical storage materials (magnesium sulfate, magnesium chloride, and calcium sulfate) with the best efficiencies due to their elevated discharge temperatures which reduce the energy consumption of membrane distillation. In addition, these materials have high volumetric energy storage density, which enables capture and transportation of waste heat from remote locations such as natural gas compressor stations to the well sites, yielding up to 70% reduction in transportation costs relative to moving FPW to centralized treatment facilities at natural gas compressor stations. Our study, for the first time, demonstrates the importance of selecting appropriate energy storage material for leveraging low-grade thermal energy such as waste heat to power membrane distillation for decentralized wastewater treatment.

* Corresponding authors.
E-mail addresses: tiezheng.tong@colostate.edu (T. Tong), tband@colostate.edu (T.M. Bandhauer).

https://doi.org/10.1016/j.apenergy.2022.120342
Received 12 June 2022; Received in revised form 14 October 2022; Accepted 11 November 2022
Available online 24 November 2022

1. Introduction

The surge of unconventional oil and gas production in the U.S. improves national energy security and the domestic economy, but it also creates a challenge to water sustainability due to the high volumes of freshwater consumption and wastewater generation [1,2]. Unconventional oil and gas production increased water consumption for oil and gas extraction by over 700% in the United States from 2011 to 2016 [2]. Furthermore, wastewater generated within the first year of drilling increased by over 500% for the same period [2]. The Colorado Oil and Gas Conservation Commission reports an increase from 8,571,529 to 65,947,898 barrels of wastewater produced per year from 2010 to 2020 in Weld County, Colorado, representing a 670% increase [3]. The treatment and reuse of flowback and produced water (FPW) by desalination is a promising strategy for sustainable wastewater management in the oil and gas industry [4-7]. Unfortunately, reverse osmosis, the most energy-efficient membrane desalination technology, is limited in its ability to treat FPW due to its high salinity (FPW can have salinities up to 10 times those of seawater, exceeding the salinity limit of reverse osmosis) [4-12]. In order to treat high-salinity wastewater such as FPW, more energy- and cost-intensive thermal technologies such as mechanical vapor compression need to be applied [13-15]. Recently, membrane distillation (MD), a hybrid thermal-membrane technology, has attracted increasing interests for the treatment of FPW [7,14-17]. Membrane distillation requires lower temperature for operation when compared to mechanical vapor compression but is still capable of treating high-salinity brines. This feature renders MD requiring less expensive materials and capital cost than mechanical vapor compression [18,19]. However, the energy efficiency of membrane distillation is lower than mechanical vapor compression. The gain output ratio (GOR) of single-stage MD is typically in the range of 1–2, which is lower than that of mechanical vapor compression (typically 10–20) [14,17,20,21]. Thus, as an emerging technology, membrane distillation is only commercially competitive for FPW treatment if low-cost energy sources are available.

The use of waste heat (WH), an otherwise wasted energy source, has often been proposed as a promising solution that reduces the cost and carbon footprint associated with energy supply to membrane distillation desalination [13,14,19,22]. However, waste heat is not readily available for use in decentralized produced water treatment systems and requires storage or transportation to arrive in a useful state for treatment. MD is able to leverage waste heat because it requires heat sources of moderate temperature (<90 °C). Potential waste heat sources have been identified both on-site (e.g., from hydraulic fracturing) and off-site (e.g., from natural gas compressor stations) of producing well pads. Although the use of waste heat potentially achieves low-cost, decarbonized treatment of FPW, the feasibility of this strategy has yet to be holistically evaluated in practice. For example, Robbins et al. [14] recently showed that the majority of waste heat generated on the well pads only persists for a short period of time. The temporal inconsistency between waste heat availability and FPW treatment demand results in the need for long-term (>48 h) storage of waste heat for future utilization.

The consideration of waste heat storage and the relevant storage materials to overcome the temporal and spatial inconsistencies of the waste heat utilization is an interesting and necessary concept to further address in the analysis of waste heat utilization for membrane distillation powered by waste heat. When evaluating thermal storage materials, a major concern is the heat loss, which can occur for the following reasons. The first reason relates to the transfer of stored heat to surroundings at lower temperatures. Second, once the temperature of the storage materials decreases below the operating temperature of the treatment technology (i.e., MD in the current study), any additional stored heat is unusable. The difference between the initial temperature of the storage materials and the required temperature for treatment needs to be considered. Due to this temperature gap, a portion of the collected waste heat is used to heat the thermal storage material to the minimum operating temperature, rather than being used for treatment. As a result, using waste heat as an energy source may not be as easy as previous studies have assumed [13,14,19,22,23]. The effects of waste heat storage on waste heat utilization and the efficiency of membrane distillation treatment are underexplored in the literature.

Herein, this study investigates the viability of leveraging waste heat for decentralized FPW treatment using membrane distillation by performing systematic assessments through thermodynamic modelling of three waste heat utilization scenarios (Fig. 1). In the first scenario, we evaluate the storage of on-site waste heat for FPW treatment and focus on the temporal disparities between waste heat availability and FPW production. Three types of waste heat storage materials (i.e., sensible, phase-change (latent), and thermo-chemical storage materials) are considered in this scenario due to their different properties and behaviors in heat storage and release. The performance of these materials is compared by evaluating the long-term energy consumption of membrane distillation with a new metric, namely apparent specific energy consumption (ASEC) that objectively captures the potential of stored waste heat for FPW treatment. The second scenario proposes a novel approach of transporting waste heat from centralized, consistent sources such as natural gas compressor stations to the well pads for on-site treatment. This strategy avoids temporal mismatches associated with waste heat usage but is subject to spatial mismatches that require the consideration of transportation cost. The economic prospect of this approach is compared with the transportation of FPW to natural gas compressor stations for centralized treatment (i.e., the third scenario). The resultant comparison is determined by the treatment potential of the waste heat storage material (i.e., the volume of treated FPW per volume of fully charged storage material). In addition, the implications of our findings on the use of waste heat to power decentralized FPW treatment are discussed.

2. Methods

2.1. Flowback and produced water volumes and waste heat availability

The data on wells from the Denver-Julesburg Basin in Colorado were collected to provide values for FPW production rates. Using the Colorado Oil and Gas Information System database, FPW production volumes were collected for 20 random wells (Table 1) [3]. The collected values are for the first two months of production, which have been identified as a critical focus for FPW treatment efforts [14]. The values used in this study to represent the daily FPW production rate (FPW_{day}) from the 20 wells in this study range from 12.9 to 289.6 m^3/day, with an average of 68.7 m^3/day (Table 1).

There is a limited amount of waste heat available on-site once the well is operational. Therefore, this study investigates the utilization of waste heat generated from hydraulic fracturing to power FPW treatment. Data for water volumes used in hydraulic fracturing can also be found in the Colorado Oil and Gas Information System database [3]. Using these volumes, waste heat generation (WH) from hydraulic fracturing were estimated following the method used in our recent publication [14], which assumes pumping power needed and system efficiencies to quantify waste heat generation for each well (Table 1). The temperature of such waste heat is assumed to be 90 °C, which is discussed in more detail in the next section. Among the investigated wells, the Wells Ranch State well generated the highest amount of waste heat at 7,867 GJ, whereas the Markham well produced the lowest waste heat value at 1,586 GJ. The average waste heat availability from hydraulic fracturing is estimated to be 3,087 GJ and the majority (90%) of waste heat production values fall between 1500 and 4500 GJ (Table 1).

2.2. Selection of representative wells

This study analyzed 20 wells that represent the FPW treatment demand and waste heat availability in Weld County, CO [14]. There is a

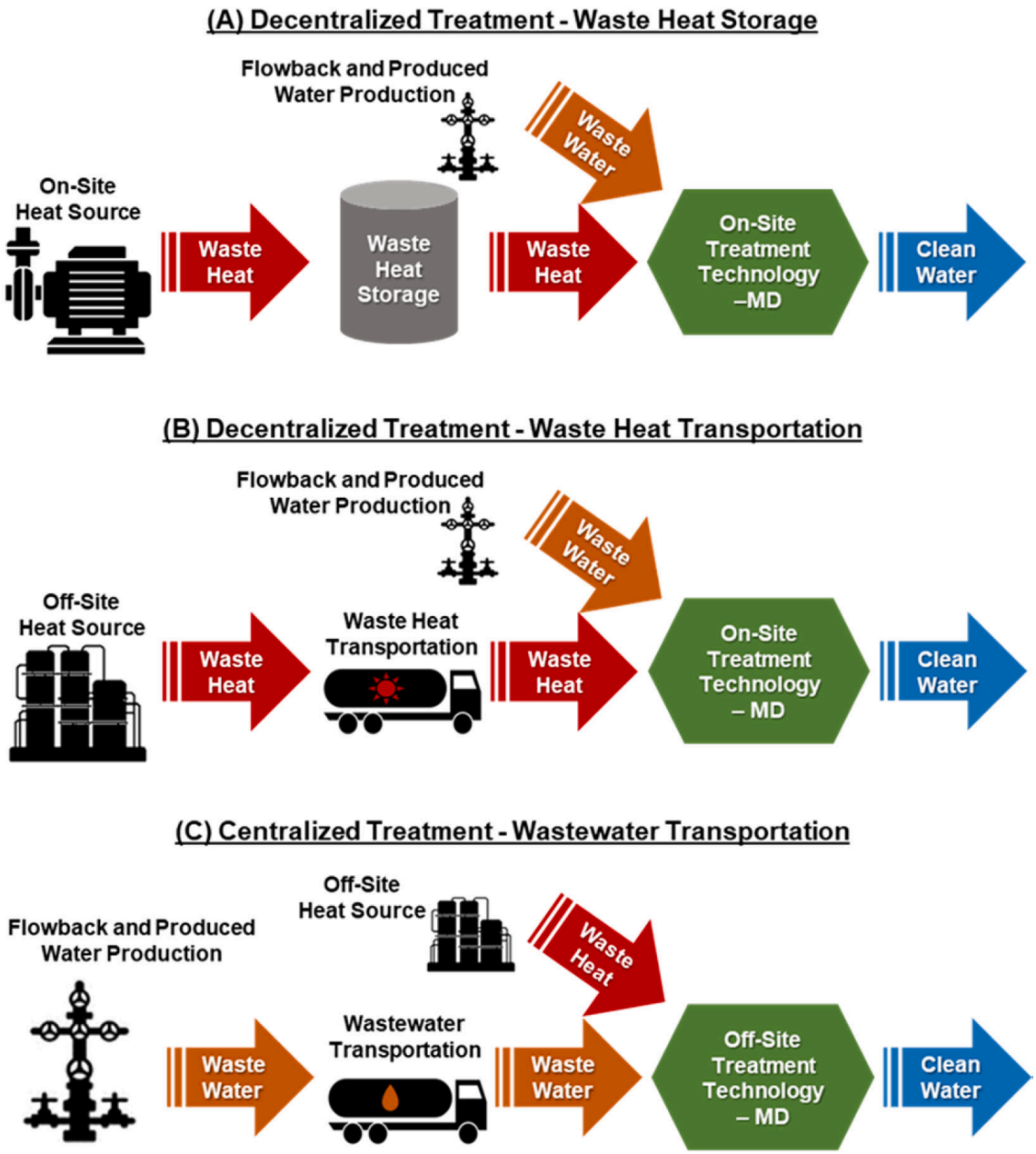

Fig. 1. Options of decentralized and centralized flowback and produced water treatment using waste heat from hydraluic fracturing processes as the on-site heat source and waste heat from natural gas compressor stations as the off-site heat source. A) Decentralized treatement using stored waste heat from hydraulic fracturing. B) Decentralized treatement using stored waste heat transported from natural gas compressor stations. C) Centralized treatment of transported flowback and produced water using waste heat at natural gas compressor stations.

large distribution of waste heat availability and FPW production, which are used to determine the minimum GOR that is required by a technology for the waste heat to be capable of meeting treatment demands at a given well (Fig. 2). The minimum GOR is determined by first multiplying the total volume of FPW generated at the well by the latent heat of vaporization for water (i.e., 2,260 kJ/kg). This value is then divided by the total waste heat availability, resulting in a non-dimensional number equal to the minimum GOR for a given well. A higher minimum GOR indicates that MD needs to have a higher energy efficiency to meet the FPW treatment demand. For example, the minimum GOR is equal to 13.3 for the Varra well. Such a high GOR is very challenging to achieve by MD technology [14,17], and thus indicates the insufficiency of waste heat to supply heat to treat all the FPW at this well. In contrast, the minimum GOR for the Peterson well is 0.8, which is reasonable to reach for MD [14,17].

This work mainly discusses the results of three wells that represent three general scenarios of utilizing waste heat for FPW treatment. For the first well (i.e., the Varra well), the ratio of available waste heat to FPW treatment demand is low, representing a conservative scenario in which waste heat is likely insufficient to treat all the FPW. For the second well (i.e., the Jaguar well), the ratio of waste heat to FPW is average and represents the average treatment scenario. For the third well (i.e., the Peterson well), there is a high ratio of waste heat available to FPW treatment demand, representing an optimistic scenario in which waste heat is likely more than sufficient to treat all the FPW. As shown in Figure 2B, the three wells we select exhibit the high-end (13.3), average (2.0), and low-end (0.8) of the minimum GOR, at the Varra, Jaguar, and Peterson wells, respectively. The results of the other 17 wells are presented in the Supporting Information but are not shared in this main text.

Table 1
Data on flowback and produced water and waste heat generation for the wells investigated in this study [3].

Well Name	Well API#	WH GJ	FPW_{day} m^3/day
Cervi	41,222	2053.87	55.8
Dukes Federal	42,981	3584.00	111.5
Ehrlich	43,541	1997.36	33.1
Hazzard Federal	42,980	1642.11	89.1
Hood	44,371	2328.68	27.1
Horsetail	41,774	2569.61	74.6
J Klein	42,999	2741.38	35.2
Jaguar	42,622	4036.25	75.7
JZM	42,666	3994.56	130.7
Markham	43,247	1585.86	123.0
Orr State	43,975	2416.89	15.1
Peterson	44,718	3057.83	21.5
Puma Fed	42,566	2589.44	26.1
RBF	44,446	2179.49	26.8
Stromberger	42,557	5828.74	12.9
TC Hiland Knolls	43,516	3750.09	60.5
Varra	39,983	2362.58	289.6
Wells Ranch State	43,879	7866.87	65.7
Wilson Ranch	41,066	2488.18	42.8
Woolley Sosa	38,110	2669.17	57.6

Waste heat values were calculated by assuming each well produces 349.3 kJ of waste heat for every gallon of water that is used during hydraulic fracturing. This assumption considers both pumping and engine efficiencies of 89% and 43%, respectively, and a required pressure increase of 41 MPa for fracturing. These assumptions are used and justified in our previous publication [14].

2.3. Selection of waste heat storage materials

Three types of materials are considered for the thermal storage of waste heat: sensible storage materials (SSMs), phase-change storage materials (PCMs), and thermo-chemical storage materials (TCMs), as shown in Tables 2 and 3. Each material type has its advantages and disadvantages for waste heat storage. SSMs are simple to evaluate because they do not change state and energy storage changes linearly with temperature. Water is the representative SSM explored in this study, which has been identified as the best SSM due to its low cost, high availability, high energy density, low environmental impact, and minimal safety hazard when compared to other SSMs [24,25].

PCMs absorb heat through a change of phase from solid to liquid while at a constant temperature (T_{pc}, Table 2). In addition to absorbing heat through the latent phase change process (Δh_{pc}, Table 2), these materials also absorb sensible heat through an increase of temperature in either the liquid or solid phase. When selecting PCMs, it is important to find materials with phase change transition temperatures relevant to the operation temperature range for MD. As shown in Table 2, PCMs investigated in the present study possess transition temperatures ranging between 54 °C and 69 °C, which lies within the 40–90 °C operating range of membrane distillation used in this study.

TCMs were considered for their advantages of low heat loss during long-term storage (>48 h) and their high energy density [32]. Due to their high energy density, all TCMs considered in this study store energy through chemical or physical sorption processes with water, which absorbs into a liquid or adsorbs on the surface of the storage material during energy storage [33,34]. In general, these processes desorb water in the gas phase (sorbate) from the sorbent material when heat is applied during the charging mode, and then adsorb water vapor in the sorbent to

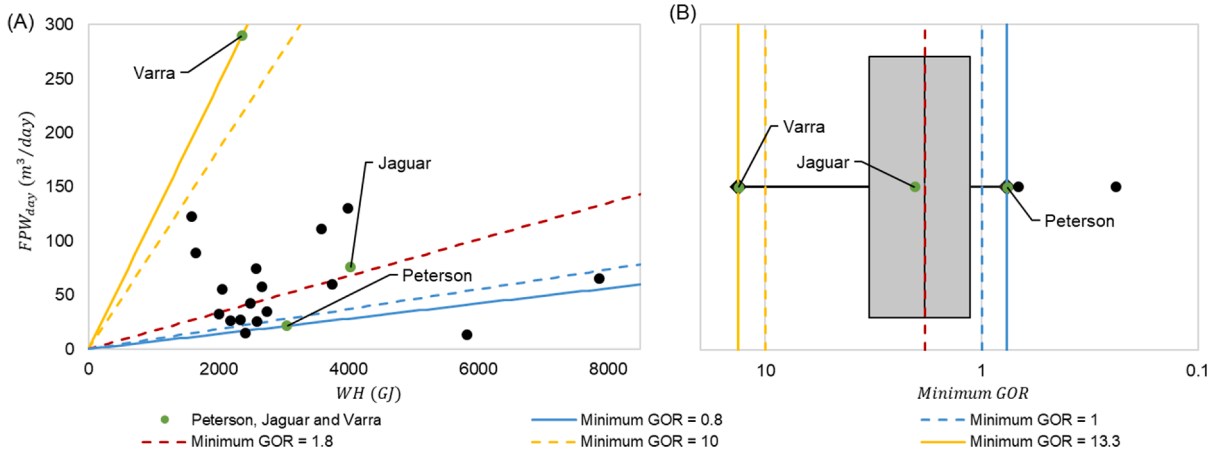

Fig. 2. (A) A plot comparing daily flowback and produced water production and total waste heat generation of each well from Table 1. (B) Distribution of the minimum GOR needed for the waste heat availability to meet treatment demands for the same 20 wells. The first quartile value is 0.8, median value is 1.8 and third quartile number is 13.3.

Table 2
Properties of sensible and phase change material for waste heat storage considered in this study.

Storage Material	Type	ρ kg/m^3	T_{pc} $°C$	Δh_{pc} kJ/kg	ΔH kJ/kg	$E_{density}$ MJ/m^3	References
Water	SSM	965	–	–	293	283	[26]
Paraffin Wax	PCM	670	56	143	282	189	[27]
n-Pentacosane	PCM	801	54	238	395	317	[28]
n-Hexacozane	PCM	803	56	256	419	336	[28]
n-Heptacozane	PCM	779	59	235	387	301	[28]
n-Nonacozane	PCM	808	63	239	405	327	[29]
n-Triacontane	PCM	775	65	252	410	318	[29]
Myristic Acid	PCM	860	54	190	349	300	[30]
Palmitic Acid	PCM	850	64	185	334	284	[28]
Stearic Acid	PCM	940	69	209	354	333	[31]

Table 3
Thermo-chemical waste heat storage materials that use water as the sorbate.

Sorbent	Type	T_{charge} °C	T_{dis} °C	$E_{density}$ MJ/m^3	References
Lithium Bromide	Liquid Absorbent	81	40	1127	[32,34,38]
Lithium Chloride	Liquid Absorbent	66	66*	1440	[32,38]
Potassium Hydroxide	Liquid Absorbent	63	63*	1127	[32,38]
Sodium Hydroxide	Liquid Absorbent	98	63	727	[32,34,38]
Calcium Sulfate	Chemical Adsorbent	150	89	1400	[33,39]
Magnesium Chloride	Chemical Adsorbent	130	100	2001	[32,35,38]
Magnesium Sulfate	Chemical Adsorbent	150	111	3063	[32,33,35,38]
Silica Gel	Solid Physical Adsorbent	88	70	180	[32,34]
Zeolite 13X	Solid Physical Adsorbent	173	63	547	[32,34]
Zeolite 13XBF	Solid Physical Adsorbent	150	75	277	[32,34]
Zeolite 4A	Solid Physical Adsorbent	205	60	384	[32,34]

Materials with charging temperature above the temperature of available waste heat will result in the material not being charged. The assumption made that all waste heat is available at 90 °C makes some of these thermo-chemical storage materials infeasable. However, these materails are still included in this analysis, in the case that waste heat above 90 °C is available.
*The discharge temperature for lithium chloride and potassium hydroxide were not provided, and therefore are assumed to be equal to the charging temperature.

release heat in the discharge phase. In the present study, several materials were evaluated, including liquid absorbents (LiBr, LiCl, KOH, and NaOH), solid chemical adsorbents ($CaSO_4$, $MgSO_4$, $MgCl_2$), and solid physical adsorbents (silica gel and zeolites) (Table 3). The configuration of the energy storage system can be theoretically complex, and there have been prior investigations that have developed system concepts using a variety of TCMs [32-37]. In these systems, the charging temperature during energy storage is higher than the discharge temperature, and discharge temperatures can vary with a variety of factors, including the leveling-off of saturation of sorbate, the flowrate of inlet sorbate, etc. [25,32-37]. Conservatively, this study assumes that the heat will be delivered to the membrane distillation system at a constant temperature throughout the discharge process.

Charging temperature, discharging temperature, and the energy density of each TCM used in the present study were obtained from each provided reference in Table 3. If a range of values were given by one reference, the maximum charging temperature and the minimum discharge temperature were used. The values collected for each material were then averaged to provide the values given in Table 3. In addition, the energy density of each system includes both the sorbent and the sorbate.

Waste heat is collected from coolant and exhaust flows from engines. Heat rejected from coolant does not go over the boiling point of water. Heat rejected through the exhaust stream of an engine can be much hotter. As such, waste heat available for collection could be higher than 90 °C [13,19]. However, as discussed in previous and following sections, the waste heat source temperature is assumed to be 90 °C for this study because the maximum operating temperature of the MD treatment system is 90 °C. Some TCMs shown in Table 3 (i.e., NaOH, $CaSO_4$, $MgSO_4$, $MgCl_2$, and zeolites) have charge temperatures much higher than 90 °C. These TCMs are included because there are waste heat sources that could exceed the recorded charging temperatures (e.g., exhaust gases from gas turbines and reciprocating engines). Thus, 90 °C is used as the waste heat delivery temperature for TCMs and for the maximum charging temperature of SSMs and PCMs to result in an analysis between these different options. If a waste heat source with a higher temperature is used, more favorable results would be seen.

Visualization of the impact that each thermal storage material can have on storage and utilization of waste heat are provided in Figure 3. All SSMs and PCMs start at an initial storage temperature (typically ambient temperature), which is assumed to be 20 °C in this study. Energy storage in SSMs increase linearly as more heat is added until the temperature reaches the heat source temperature. As heat is removed from SSMs, their temperatures will decrease linearly until reaching the minimum operating temperature of membrane distillation (40 °C or 60 °C, defined as the critical operating temperature).

Similarly, PCMs also have a linear relationship between temperature and energy content at the beginning of energy storage, but once their phase transition temperature (T_{pc}) is reached, the temperature of the storage material remains constant while energy is added or removed. The amount of energy that can be removed in this constant temperature range is the latent heat, listed in Table 2 as Δh_{pc}. After the phase change process completes, the linear relationship between energy stored and temperature continues. PCMs are heated to the heat source temperature during charging and cooled to the critical operating temperature during discharge.

Sorption allows TCMs to be charged (desorbed) by a high temperature (T_{charge}; Table 3) dry flow, which removes the sorbate from the host material. The energy potential of the host material will stay high so long as it is not exposed to the sorbate (water). To recover the stored energy, water vapor is introduced to the sorbent, which ab/adsorbs and releases energy at the desired temperature. This energy is rejected to a fluid that collects the heat released at the temperature used for membrane distillation (T_{dis}; Table 3). Although this temperature can drop over time, it is assumed for this study that TCMs discharge to the fluid at a constant temperature, which is chosen conservatively [25,32-37]. This could be an advantage if the discharge temperature is high, but the overall performance could be hindered if the discharge temperature is low. This consideration will be discussed further in Section 2.4.

To capture the effect of the critical operating temperature (i.e., the minimum temperature for MD operation) on waste heat utilization viability, the critical operating temperature is assumed to be either 40 °C or 60 °C in this study. As the critical operating temperature increases, the amount of heat that can be removed from the storage material decreases. Therefore, higher critical operating temperatures decrease waste heat utilization. Moreover, the critical operating temperature directly determines the critical temperature gap, which is the difference between initial storage material temperature and the critical operating temperature. As the critical temperature gap increases, the amount of heat added to the storage material which cannot be used for FPW treatment increases. The impact of the critical temperature gap is higher in SSMs than PCMs and non-existent for TCMs. However, a lower critical operating temperature results in operation of thermally driven treatment technologies at lower energy efficiencies [14,17,22]. TCMs are not affected by the critical temperature gap because the temperature of TCMs does not determine the temperature of the fluid charging and discharging the material and as a result, the fluid is assumed to remain at a constant temperature.

2.4. Impact of waste heat temperature on membrane distillation treatment performance

It is known that for membrane distillation treatment, the temperature of the heat source (T) (assuming a constant permeate temperature) affects the specific energy consumption (SEC), distillate production rate ($\dot{m}_{clean}$), and feedwater treatment rate ($\dot{V}_{treat}$) [14,17,40-42]. To evaluate the performance of MD modules, the model of MD developed in our recently published study was used to provide a relationship between these parameters [13]. For a feedwater temperature ranging from 40 to

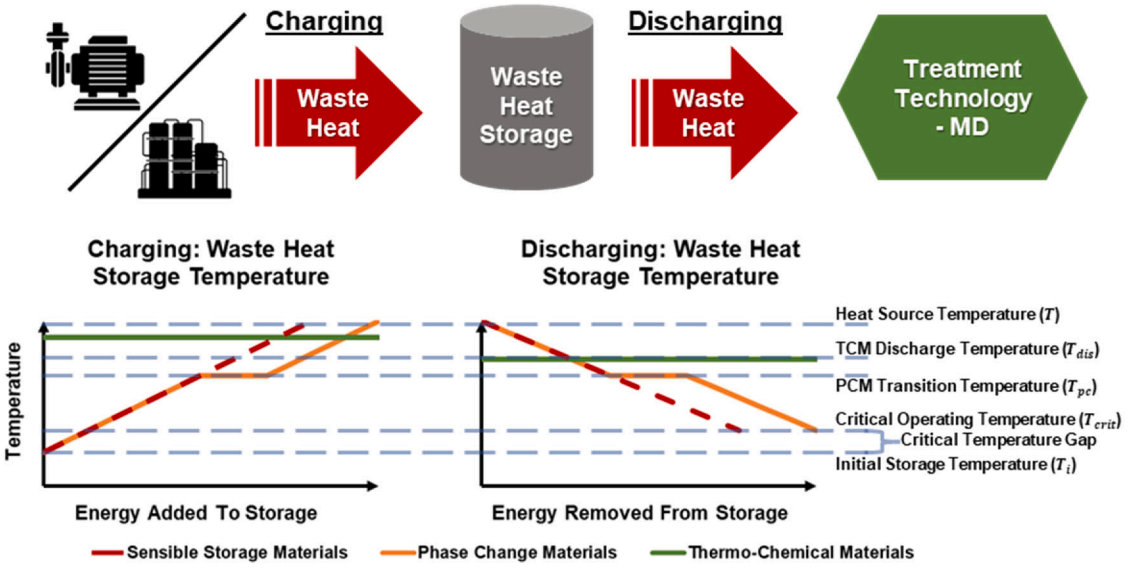

Fig. 3. Temperature variance of storage materials given waste heat source temperature, initial temperature of storage material, and critical operating temperature of membrane distillation for a sensible storage material (red), phase change storage material (orange), and thermo-chemical storage material (green). (For interpretation of the references to color in this figure legend, the reader is referred to the web version of this article.)

90 °C, SEC (i.e., the amount of energy used per kilogram of clean water produced) values ranged from 4,369 to 940 kJ/kg (Table S1, Supporting Information), which are consistent with the values reported in the literature [13,43-45].

As energy is extracted from the stored waste heat, the temperature of the storage material can decrease. Consequently, the FPW treatment efficiency of membrane distillation will decrease with time as the storage temperature drops. Steady state performance of MD can be characterized by SEC, which yields the amount of energy used per unit of distillate produced at a fixed temperature. However, because waste heat extraction causes the heat source delivery temperature to change, energy required to drive the MD process changes. The apparent SEC (ASEC) accounts for the waste heat delivery temperature change with time by determining the total amount of energy utilized (WH_{util}) to produce distillate over the full operation lifetime of the treatment technology (FPW_{clean}; Eq. 1).

$$ASEC = \frac{WH_{util}}{FPW_{clean}} \tag{1}$$

2.5. Modelling of waste heat utilization and storage

There are two distinct steps in modelling waste heat utilization: the charging and the discharging phases. During the charging phase, waste heat is collected from a source (e.g., the hydraulic fracturing process) and added to the storage material. During the discharging phase, heat is removed from the storage material to power MD for FPW treatment. Each phase is discussed in the following sections.

2.5.1. Charging storage materials with collected waste heat

The number of membrane distillation modules used at a given well (N), mass of the storage materials (m_{store}), and volume of the storage material (V_{store}) were calculated at the beginning of each system model. Multiple MD modules are needed for treatment because of the limited treatment capacity of a single MD module. To ensure a reasonable comparison between wells, the number of MD modules is only dependent on the FPW production rate at a well (FPW_{day}; Table 1) and the maximum treatment rate of a single MD module (i.e., $\dot{V}_{treat}$ at the maximum feedwater temperature; Table S1; Eq. 2). The calculation is rounded up to the nearest number of full modules. With N modules at the well and a sufficiently high temperature heat source, membrane distillation could potentially treat all FPW at the well.

$$N = roundup\left(\frac{FPW_{day}}{\max\left(\dot{V}_{treat}\right)}\right) \tag{2}$$

The mass and volume of storage materials needed to capture the waste heat from hydraulic fracturing (WH; Table 1) are unique to the well and waste heat storage material (Eqs. 3 and 4). Properties of each material can be found in Table 2 and Table 3. For SSMs and PCMs, the change in enthalpy from ambient to maximum membrane distillation temperature (ΔH) determined the required mass of the storage material. ΔH is equal to the difference between enthalpies (h) for the material at its initial temperature (T_i) before charging and the temperature of the heat source (Eq. 3.2). In this case, the temperature of the heat source is assumed to be 90 °C for SSMs and PCMs and is identical to the high temperature limit for operation of MD (T_{high}). Because neither charge nor discharge performance of the TCMs depend on mass, the mass of this storage material is not needed or calculated.

$$m_{store} = \frac{WH}{\Delta H} \tag{3.1}$$

$$\Delta H = h\left(T_{high}\right) - h\left(T_i\right) \tag{3.2}$$

The energy density ($E_{density}$) of the thermal storage materials was used to determine the needed volume of storage material (Eq. 4.1). For SSMs and PCMs, $E_{density}$ is identical to the change in enthalpy from T_i to T_{high} multiplied by the density of the material (ρ; Eq. 4.2). Because there is no temperature change within TCMs, the same method cannot be used for calculating energy density. For TCMs, the energy density is a value given in the literature based on the potential for reactions within a representatively designed system. These values are recorded in Table 3.

$$V_{store} = \frac{WH}{E_{density}} \tag{4.1}$$

$$E_{density} = \Delta H^{*}\rho \tag{4.2}$$

Alternatively, volume of the storage material can be calculated by dividing the mass of the storage material by the material density. An example calculation for the charging model is done for each storage material type in Table S2 (in the Supporting Information) for the Jaguar

well. Comparison of the needed volume of storage material shows that the energy density of a material has a significant effect on the volume of storage material. The volume of the storage material is important because storage tanks are significantly more expensive as they become larger. Therefore, the goal is to maximize energy density so that the storage material volume, as well as the corresponding storage container size, can be minimized.

2.5.2. Discharging storage materials for treatment

The steady state operating conditions for membrane distillation in Table S1 were used to calculate treatment system performance as the temperature of the stored waste heat changes. The model considers the system in discretized time portions (Δt) of 0.1 days. Energy extracted from the stored waste heat was assumed equal to the amount of heat supplied to MD for treatment at a given operating condition. This model tracks the temperature drop of SSMs and PCMs as heat is extracted from the system. The model is run until either the temperature of storage material has dropped to the critical operating temperature of the membrane distillation module ($T_{crit-low} = 40^{\circ}C$ or $T_{crit-high} = 60^{\circ}C$), all the FPW volume was treated, or all the waste heat was used. Two critical operating temperatures were considered to determine its impact on treatment and waste heat utilization. The beginning temperature of the storage material is assumed to be 90 °C. TCMs do not change temperature as heat is removed from them, so there is no need for the calculation of new system temperatures. This also means that the system performance will not change over time. Constant performance could be advantageous if the discharge temperature of the system is higher, as efficiency of the system is relatively low at lower discharge temperatures (i.e., more energy will be used to treat FPW, and it will take longer to create similar volumes of distillate).

The amount of energy removed from the thermal storage material at any point in time ($\dot{E}$) is equal to the amount of energy consumed by N membrane distillation modules at the current temperature of the storage material (T) (Eq. 5). Because the energy consumption at any moment is represented with SEC ($SEC(T)$), the distillate production rate ($\dot{m}_{clean}(T)$) is also calculated from Table S1 to determine energy consumption of the system.

$$\dot{E} = N^{*}SEC(T)^{*}\dot{m}_{clean}(T) \tag{5}$$

There is also a significant amount of heat lost to the atmosphere while in storage ($\dot{Q}_{loss}$). This loss is calculated by assuming a 10-meter-tall tank is used to store the waste heat which is insulated with 5 cm of fiberglass insulation, which has a thermal conductivity of 0.04 $W/m^{*}K$, and a heat transfer coefficient of 10 $W/m^{2*}K$ [26,46]. The diameter of the tank is determined by the necessary volume of the tank, as calculated above (Eq. 4.1). The thermal resistance of the tank walls (Res_{ins}) were determined, and the incremental heat loss was calculated (Eq. 6).

$$\dot{Q}_{loss} = (T - T_i)/Res_{ins} \tag{6}$$

This energy is removed from the thermal storage material, lowering the enthalpy of the remaining material based on Eq. 7.

$$\Delta h = -((\dot{E} + \dot{Q}_{loss})^{*}\Delta t)/m_{store} \tag{7}$$

With this rate of energy extracted, the new temperature of the storage material (T_{new}) can be calculated based on the amount of energy that has been removed from the storage material. The change in temperature is based on the current temperature of the storage material and the type of material being evaluated. For SSMs, only Eq. 8a is needed because there is no phase change. The change in temperature is equal to the change in enthalpy of the system divided by the specific heat of the storage material (c_p), which is assumed constant within phases. PCMs require the use of conditional functions. Phase change will only occur in PCMs when the temperature of the system is equal to the phase change temperature (T_{pc}). If the current temperature of the system is not equal to the phase change temperature, the system is evaluated using the same methods as for SSMs (Eq. 8a). Once the phase change temperature is reached, heat continues to be removed until the phase change is complete, without changing the temperature (Eq. 8b). Once phase change is completed, the PCM will continue to drop in temperature until the critical operating temperature is reached (Eq. 8a). The liquid fraction (x_{pc}) change is tracked through Eq. 9. The liquid fraction is equal to 1 when the PCM is in the liquid phase, or when its temperature is above the phase change temperature (Eq. 10a). When the temperature of the PCM is below the phase change temperature, the liquid fraction is 0 (Eq. 10b).

$$T_{new} - T = \begin{cases} a)\ \dfrac{\Delta h}{c_p} & T \neq T_{pc} \\ b)\ 0 & T = T_{pc}\ and\ 0 < x_{pc} < 1 \end{cases} \tag{8}$$

$$\Delta x_{pc} = \begin{cases} a)\ 0 & T \neq T_{pc} \\ b)\ \dfrac{\Delta h^{*} m_{store}}{\Delta h_{pc}} & T = T_{pc} \end{cases} \tag{9}$$

$$x_{pc} = \begin{cases} a)\ 1 & T > T_{pc} \\ b)\ 0 & T < T_{pc} \end{cases} \tag{10}$$

Waste heat utilization (WH_{util}) is calculated using Eq. 11. This will return the total amount of waste heat removed from storage for FPW treatment.

$$WH_{util} = \int_0^t \dot{E} dt \tag{11}$$

Similarly, the amount of flowback and produced water treated (FPW_{treat}) and the amount of clean water produced (FPW_{clean}) are tracked throughout the model.

$$FPW_{treat} = \int_0^t \dot{V}_{treat} dt \tag{12}$$

$$FPW_{clean} = \int_0^t \dot{m}_{clean} dt \tag{13}$$

2.6. Transport of Off-Site waste heat sources

In addition to the use of waste heat generated on-site from hydraulic fracturing, this study also evaluates the potential of off-site waste heat sources for FPW treatment. The most promising off-site waste heat source has been identified as natural gas compressor stations [13,14,19,23]. These pumping stations are very large and operate continuously. Earlier research on oil and gas production in the Denver-Julesburg Basin has shown that upwards of 70% of natural gas compressor stations would supply sufficient waste heat for FPW treatment after distance optimization [23]. It is also an important consideration that as oil and gas production increases within a specific area, the amount of waste heat from the growing number of natural gas compressor stations will increase and meet rising demands for FPW treatment. Furthermore, the temperature of the waste heat is likewise conservatively approximated to 90 °C for SSMs and PCMs.

The challenge in utilization of waste heat from natural gas compressors stations is the spatial disparity between waste heat availability and FPW production. Therefore, either the waste heat must be transported to the well (Fig. 1B) or the FPW must be transported to natural gas compressor stations (Fig. 1C) for treatment. The number of trucks needed for the transportation of storage material (Eq. 14) and FPW (Eq. 15) were calculated for each storage material and well combination based on a given truck volume (V_{truck}) of 6,000 *gallons* [47].

$$\text{Trucks for Storage Material} = \max\left(\frac{V_{store}}{V_{truck}}, X_w \frac{V_{store}}{V_{truck}}\right) \tag{14}$$

$$\text{Trucks for FPW} = \frac{FPW_{\text{treat}}}{V_{\text{truck}}} \tag{15}$$

The potential economic prospects of these two options can be compared on both a volumetric and weight basis. The distance between the well and natural gas compressor station is constant, but the number of trucks needed for transporting FPW and storage material vary. The ratio of storage material volume to the volume of treated FPW is calculated using Eq. 16. When this ratio is above 1, it requires more trucks to transport waste heat to a producing well than transporting FPW to a natural gas compressor station. However, this is based only on a volumetric consideration. The additional consideration of weight is needed to determine the actual total number of trucks needed for transportation of waste heat.

$$\text{Volumertric Ratio} = \frac{V_{\text{store}}}{FPW_{\text{treat}}} \tag{16}$$

In the scenarios where volumetric treatment capacity of a material allows for transportation of waste heat, the additional step is taken to determine the weight of the material. This is done by determining a multiplication factor (X_w) for each material that transforms the number of trucks needed based on volume to the number of trucks needed based on mass. The methods for determining this multiplication factor are discussed in Section 3 of the Supporting Information. By adding this consideration, we can now calculate the transportation ratio (Eq. 17). When the transportation ratio is below 1, it takes less trucks to transport waste heat to wells than to move FPW to natural gas compressor stations. In such scenarios, the transportation of waste heat to the producing well is economically more favorable by reducing the transportation cost.

$$\text{Transportation Ratio} = \frac{\text{Trucks for Storage Material}}{\text{Trucks for FPW}} \tag{17}$$

3. Results

3.1. Utilization of waste heat for the treatment of produced water

The operation of MD determines the efficiencies of both waste heat utilization and FPW treatment, which are also dependent on the storage materials being used. FPW treatment will stop when the storage material has reached the critical operating temperature, all the FPW has been treated, or all the available waste heat has been consumed. It can be determined which of these criteria is reached first by observing Figures 4, 5, and 6. In these sets of graphs, the fraction of waste heat utilization (top) and fraction of FPW treated (bottom) are tracked along the delivery temperature of stored heat from SSMs (A), PCMs (B), and TCMs (C). The critical operating temperature of 40 °C is shown for SSMs and PCMs, which helps determine when treatment is concluded due to insufficient temperatures (e.g., Fig. 5A). For the sake of not overcrowding the figures, not all PCMs or TCMs are shown. The materials shown in the main text were selected to show the range of phase change and discharge temperatures of the materials. Results for the other materials can be found in the Supporting Information.

For the Peterson well (i.e., the optimistic scenario for treatment), using water as a thermal storage material did not reach full waste heat utilization nor did the system reach full FPW treatment (Fig. 4A). Therefore, the storage system had to have met the critical operating temperature of membrane distillation. Though most of the PCMs near full treatment, only stearic acid achieves full treatment. TCMs are more

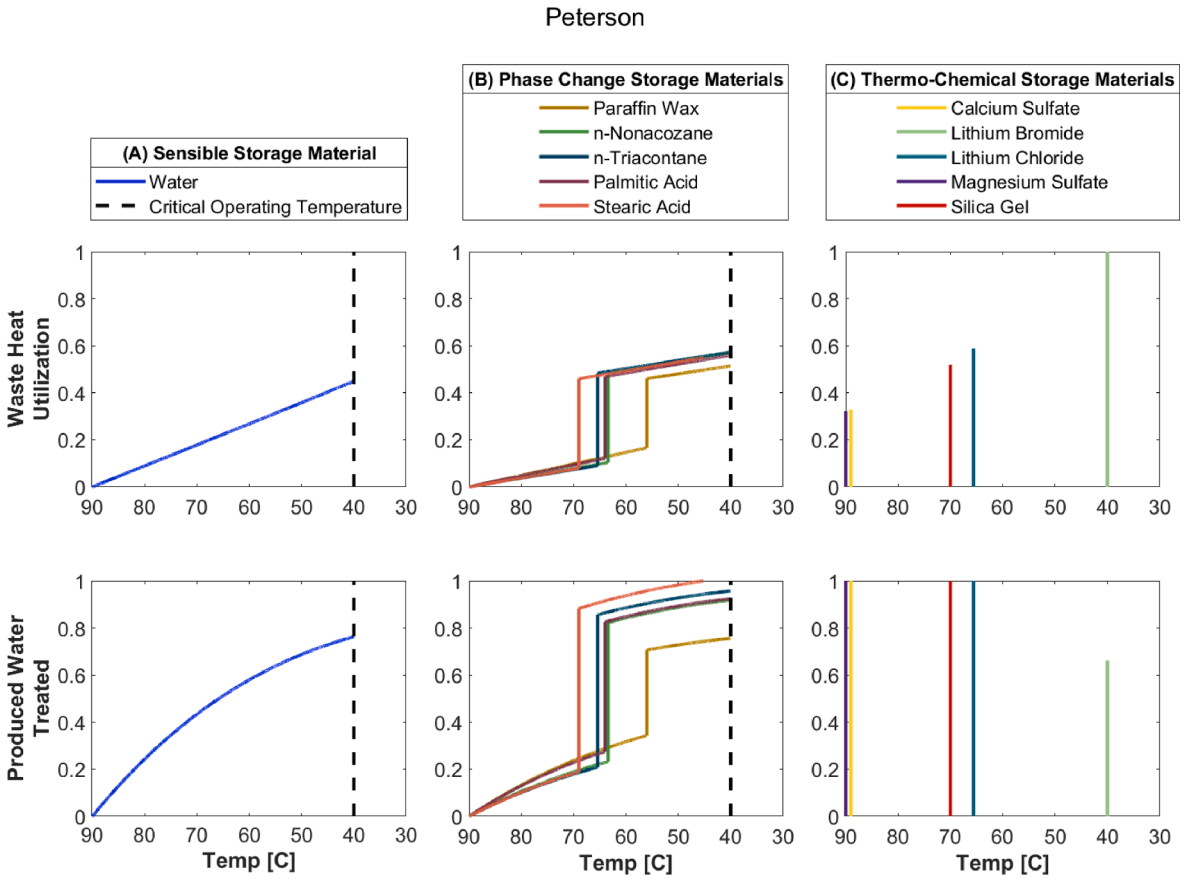

Fig. 4. Utilization of waste heat (top) and flowback and produced water treated (bottom) in relation to the storage material temperature for sensible (A), phase-change (B), and thermo-chemical (C) storage materials at the Peterson well, the optimistic treatment scenario. The fraction of waste heat utilization and fraction of flowback and produced water treated are tracked along the delivery temperature of heat from the storage matierals.

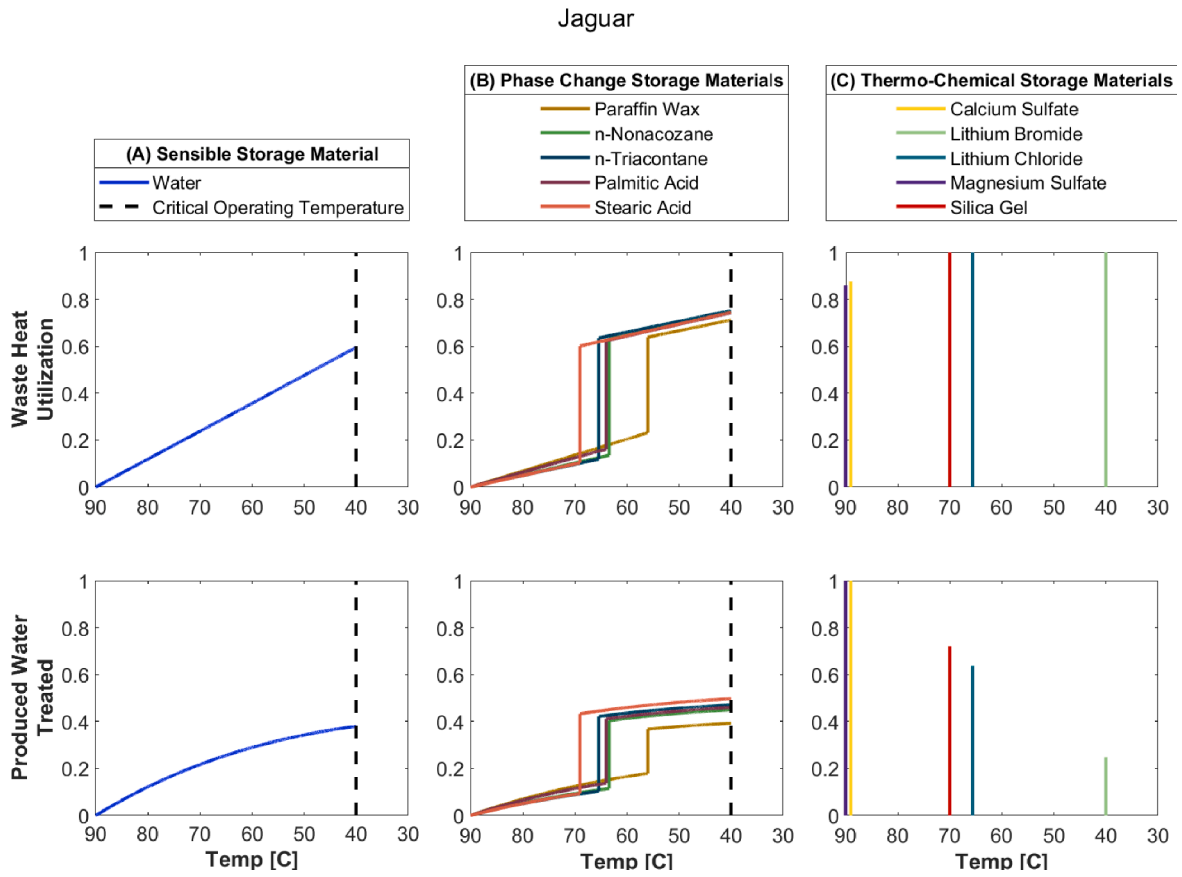

Fig. 5. Utilization of waste heat (top) and flowback and produced water treated (bottom) in relation to the storage material temperature for sensible (A), phase-change (B), and thermo-chemical (C) storage materials at the Jaguar well, the average treatment scenario. The fraction of waste heat utilization and fraction of flowback and produced water treated are tracked along the delivery temperature of heat from the storage matierals.

successful. The only TCM that does not result in full treatment at the Peterson well is lithium bromide which enables 66% treatment (Fig. 4C). Because lithium bromide has a very low discharge temperature (close to the critical operating temperature of MD, Table 3), the system operates at low performance in terms of both energy efficiency and treatment capacity.

The Jaguar well, which represents the average scenario, has less favorable results for FPW treatment compared to the optimistic Peterson well. For most storage materials being used at this well, FPW treatment demand is not met (i.e., less than 100% FPW is treated) and waste heat is extracted from the storage material until the critical operating temperature is reached (Fig. 5). For example, with a critical operating temperature at 40 °C, 37%-50% of FPW is treated when SSM (i.e., water in this study) and PCMs are used, with 60%-75% of waste heat utilized (Fig. 5A and Fig. 5B). However, when TCMs are used, 86%-100% of waste heat is utilized to treat 25%-100% of FPW (Fig. 5C). The materials achieving 100% FPW treatment at this well include magnesium sulfate, magnesium chloride, and calcium sulfate, which are concluded later in this work to be the best options for waste heat storage for FPW treatment. Furthermore, Figure 6 shows results for the conservative scenario (i.e., the Varra well). Due to the high amount of FPW generated at this well, only a small fraction of FPW is treated when the storage materials reach the critical operating temperature, regardless of the materials used for waste heat storage. Therefore, the waste heat generated from hydraulic fracturing on-site is not meeting the treatment demand of FPW in such a scenario.

Among the 20 wells evaluated by this study, 1 well, Stromberger, experienced 100% treatment of FPW for all storage materials. The Stromberger well performs better than the average levels, thereby representing the optimistic scenario. At 4 wells, 100% FPW treatment is only possible when TCMs with very high discharge temperatures are used (i.e., calcium sulfate, magnesium sulfate, and magnesium chloride). Also, 7 wells have below-average results, where 100% FPW treatment is not possible, no matter which storage material is used. Additionally, 13 wells have results showing that at least one storage material provides possibility for 100% FPW treatment. All the findings above are distilled from the results from the 20 wells investigated in this study (3 wells shown in the main text and 17 wells summarized in the Supporting Information).

The difference among the storage material types for waste heat utilization can be further investigated. The constant decrease in temperature for a SSM is a disadvantage that results in lower performance (i.e., higher energy consumption to produce similar volumes of water) over the treatment period (Fig. 5). In contrast, PCMs can take advantage of constant temperatures during heat transfer in latent heat ranges. Even further, TCMs operate at constant temperature at all times, rendering TCMs with high discharge temperatures outperforming both SSMs and PCMs. Using the baseline case at the Jaguar well as an example, the use of water as the storage material resulted in the system to treat 38% of FPW when the critical operating temperature is 40 °C (Fig. 5A). At the same critical operating temperature, the use of PCMs results in 37%-50% of FPW being treated (Fig. 5B). By taking advantage of constant temperature during discharge, TCMs are capable of meeting 54–100% treatment demand when excluding lithium bromide (Fig. 5C).

The transition temperature of PCMs and the discharge temperature of TCMs play important roles in determining the energy consumption and treatment capacity of MD systems coupled with thermal energy storage. As stated earlier, MD treatment performs better (i.e., with lower energy consumption and higher treatment rates) when the temperature of the waste heat storage material is higher. In the Peterson well, for

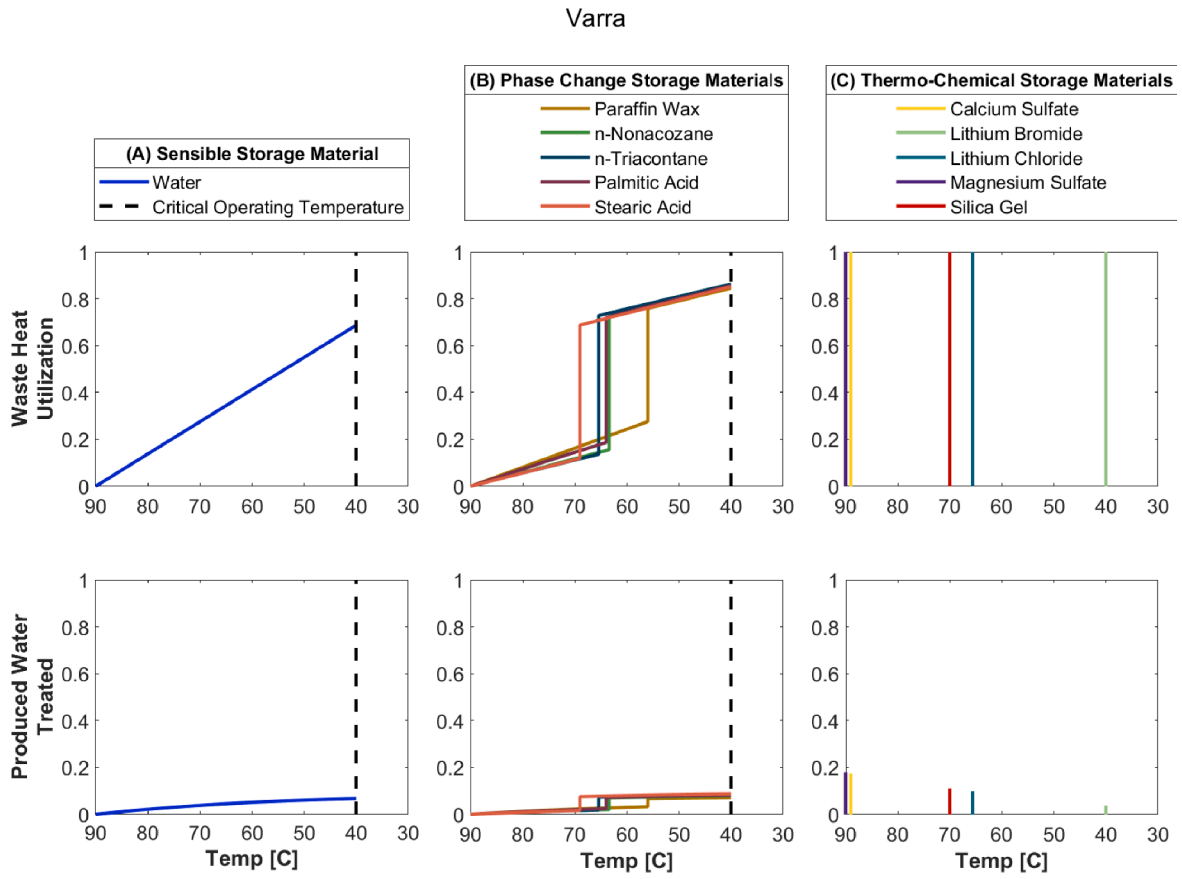

Fig. 6. Utilization of waste heat (top) and flowback and produced water treated (bottom) in relation to the storage material temperature for sensible (A), phase-change (B), and thermo-chemical (C) storage materials at the Varra well, the conservative treatment scenario. The fraction of waste heat utilization and fraction of flowback and produced water treated are tracked along the delivery temperature of heat from the storage matierals.

example, each of the TCMs, excluding lithium bromide, supply heat to treat the full amount of FPW without using the full potential of stored waste heat (Fig. 4). Additionally, PCMs result in very close to full treatment. However, the utilization of waste heat increases as the transition temperature of the PCMs or the discharge temperature of the TCMs lowers (Fig. 4). Because each of these scenarios are treating the same amount of FPW, normalized energy consumption of the treatment system increases as the PCM transition temperature or TCM discharge temperature decreases. This relationship arises because materials with a higher transition temperature or discharge temperature can maintain better performance of MD treatment technology (i.e., operate at higher temperatures) for longer periods. Such behaviors will be captured using the new metric (i.e., ASEC) as detailed in the next section.

As clearly shown for the Jaguar well, a higher PCM transition temperature or higher TCM discharge temperature results in a higher FPW treatment capacity by MD (Fig. 5B and Fig. 5C). For example, the use of stearic acid, which has a transition temperature of 69 °C, results in 11% more treatment than the use of paraffin wax, which has a transition temperature of 56 °C. Because all PCMs are using roughly the same amount of waste heat, and all TCMs except for calcium sulfate and magnesium sulfate have exactly the same waste heat utilization, it can be concluded that FPW treatment capacity is higher when PCM transition temperatures or TCM discharge temperatures are higher. A closer look at TCMs show that using materials with high discharge temperatures (i.e., 89 °C for calcium sulfate) could result in complete FPW treatment as compared to 25% of FPW treatment when using a TCM with lower discharge temperature (i.e., 40 °C for lithium bromide). These relationships are not limited to the Jaguar well. Higher PCM transition temperatures and higher TCM discharge temperatures result in higher treatment capacities and lower energy consumption of MD per unit of clean water produced (i.e., having lower ASEC values) for all the wells investigated in this study.

The above analyses show that when waste heat is not sufficient to treat all the FPW (e.g., for the Jaguar and Varra wells), not all the available waste heat could be utilized for treatment using SSMs or PCMs due to the presence of a critical operating temperature. The critical operating temperature, and subsequently the critical temperature gap (Fig. 3), drop the maximum waste heat utilization when using waste heat storage materials. As critical temperature gaps become larger, more energy is being dedicated to the pre-heating of the storage material to the critical operating temperature, rather than MD treatment. This energy is lost to the system and removes a portion of the available waste heat for utilization. As a result, each SSM and PCM has a maximum waste heat utilization, which is a property of the system based on both the material being used and the critical operating temperature (Table 4). It is also worth mentioning that the maximum waste heat utilization is a function of MD operational condition and waste heat storage material, but it does not change from well to well.

The transition temperature of PCMs and the discharge temperature of TCMs are also important when considering the critical operating temperature of MD. When the critical operating temperature is higher, some PCMs, with transition temperatures below the critical operating temperature, utilize less waste heat than SSMs (i.e., water) because they are no longer able to store latent heat through phase change and are only leveraging sensible heat (Table 4). For example, at a higher critical operating temperature of 60 °C, some PCMs (i.e., paraffin wax, n-pentacosane, n-hexacozane, n-heptacozane, and myristic acid), which have transition temperatures below the critical operating temperature, have low maximum waste heat utilization which ranges from 17 to 26%, while using water as the storage material achieves a higher waste heat

Table 4
Maximum waste heat utilization for all materials given the two different critical operating temperatures.

Material	Maximum WH_{util} (%)	
	$T_{crit} = 40^{\circ}C$	$T_{crit} = 60^{\circ}C$
Water	**71**	**43**
Paraffin Wax*	**89**	**26**
n-Pentacosane*	**89**	**17**
n-Hexacozane*	**89**	**17**
n-Heptacozane*	**89**	**17**
n-Nonacozane	**89**	**77**
n-Triacontane	**89**	**79**
Myristic Acid*	**87**	**19**
Palmitic Acid	**89**	**77**
Stearic Acid	**88**	**77**
Calcium Sulfate	**100**	**100**
Lithium Bromide*	**100**	**0**
Lithium Chloride	**100**	**100**
Magnesium Chloride	**100**	**100**
Magnesium Sulfate	**100**	**100**
Potassium Hydroxide	**100**	**100**
Silica Gel	**100**	**100**
Sodium Hydroxide	**100**	**100**
Zeolite 13X	**100**	**100**
Zeolite 13XBF	**100**	**100**
Zeolite 4A	**100**	**100**

*These accented waste heat storage materials have PCM transition temperatures or TCM discharge temperatures below the higher critical operating temperature of 60 °C.

utilization (43%). Meanwhile, the remaining PCMs (i.e., n-nonacozane, n-triacontane, palmitic acid, and stearic acid), which have transition temperatures above the critical operating temperature, result in waste heat utilization ranges from 77 to 79%. This is another reason that PCMs with higher transition temperatures are of more interest in waste heat storage for flowback and produced water treatment. Furthermore, some TCMs (e.g., lithium bromide) may not be feasible options when higher critical operating temperatures are used, because the discharge temperature is lower than the critical operating temperature. It is worth mentioning that having a lower maximum waste heat utilization does not mean that complete treatment of FPW is impossible. This is especially true in scenarios where there is abundant waste heat available to meet treatment demands.

3.2. Apparent specific energy consumption

Although waste heat utilization and treated FPW volumes are important metrics, the ASEC, for the first time, takes both into account and indicates the total treatment system performance when leveraging waste heat to power membrane distillation treatment. The ASEC, which is defined as the total amount of waste heat utilized per kilogram of clean water produced, is calculated by generalizing the total energy used and total clean water produced throughout the lifetime of the treatment system (Eq. 1). The ASEC of membrane distillation when using each storage material was calculated at each well for the range of critical operating temperatures from 40 °C to 60 °C (Fig. 7). As shown in Figure 7, SSMs and PCMs have different ASEC values based on both the critical operating temperature and the well being evaluated. The lowest ASEC (circles) is associated with the highest critical operating temperature, and the highest ASEC is indicated by a diamond at the lower critical operating temperature. As the discharge temperature of TCMs does not change as heat is removed, the ASEC is only dependent on the material type, but not the well. The remaining ASEC data for other wells can be found in the Supporting Information (Table S4-Table S23).

In general, the ASEC values for most SSMs and PCMs (i.e., 1,365–2,251 kJ/kg) are comparable to energy consumption of systems using TCMs (i.e., 1,350–2,060 kJ/kg). This comparison excludes TCMs such as magnesium sulfate, magnesium chloride, and calcium sulfate which perform at lower ASEC values (i.e., 954–973 kJ/kg) and lithium bromide which performs at higher ASEC value (i.e., 4,483 kJ/kg) because of their high and low discharge temperatures, respectively. Yet, the three TCMs with high discharge temperatures (magnesium sulfate, magnesium chloride, and calcium sulfate) decrease ASEC by nearly 30%: a significant energy savings that make high discharge temperature TCMs more promising for waste heat storage.

By comparing the ASEC values from Figure 7 to the calculated critical (i.e., maximum) SEC at a well, it can directly be determined if the proposed treatment system will be capable of achieving complete treatment of FPW. The minimum GOR can be converted to critical SEC at any well by dividing the latent heat of vaporization for water by the minimum GOR (Fig. 2). If the ASEC is above the critical SEC, full treatment is not possible. For example, the critical SEC of the Jaguar well is 1,111 kJ/kg. By looking at the ASEC values from the Jaguar well (Fig. 7), it can be concluded that only TCMs such as magnesium sulfate, magnesium chloride, and calcium sulfate are capable of meeting the FPW treatment demands. This conclusion is confirmed in Figure 5, as only the TCMs with very high discharge temperature are capable of achieving full FPW treatment. The critical SEC of the Peterson well is 2,965 kJ/kg, and thus the only TCM that cannot reach full treatment for this well is lithium bromide, which has an ASEC of 4,483 kJ/kg.

The average critical SEC obtained from Figure 2 is 987 kJ/kg, which, in the average case, means only systems using TCMs like magnesium sulfate, magnesium chloride, and calcium sulfate (i.e., the only storage materials with ASEC values under 987 kJ/kg) would be able to meet the FPW treatment demand. For wells with below average minimum GOR values (i.e., 50% of wells), none of the treatment systems could be expected to meet FPW treatment demands by using waste heat from hydraulic fracturing. Among all the materials, only magnesium sulfate, magnesium chloride, and calcium sulfate are able to operate with ASEC values below 1000 kJ/kg. High FPW treatment and lower energy consumption are precursors to a low ASEC value, and therefore these three TCMs enable the highest performance of MD and are the best options available for waste heat storage for use in on-site FPW treatment.

3.3. Storage volumes and potential for transportation of waste heat from natural gas compressor stations

Due to the temporal disparity between on-site waste heat generation and FPW treatment demand, we consider another option of waste heat utilization for on-site FPW treatment: the transport of waste heat from natural gas compressor stations, which are more consistent waste heat sources, to the well sites. Therefore, waste heat storage materials need to be transported from the natural gas compressor stations to the well. This strategy needs to be compared to the transport of raw FPW to natural gas compressor stations for off-site treatment [13,23]. In this case, the number of trucks for the transport of storage material used for waste heat storage must be smaller than the trucks needed to transport raw FPW being treated, because the transportation cost is proportional to the number of trucks transported.

By estimating the inverse volumetric treatment capacity of storage materials for each well (Eq. 16), the viability of transporting waste heat from natural gas compressor stations for decentralized FPW treatment is determined, using the Varra, Jaguar, and Peterson wells as examples for the conservative, average, and optimistic scenarios (Fig. 8). The analyses on the remaining wells are shown in the Supporting Information (Table S4-Table S23). The majority of waste heat storage materials result in higher volumes when transporting waste heat for on-site FPW treatment, compared to transporting raw FPW to natural gas compressor stations for centralized treatment. However, three TCMs were identified with the potential to significantly reduce the transportation volume: calcium sulfate, magnesium chloride, and magnesium sulfate. In the average case (i.e., at the Jaguar well), for example, these TCMs have volumetric ratios of storage materials to treated FPW between 0.29 and 0.63. When weight is considered, the transportation ratios for these

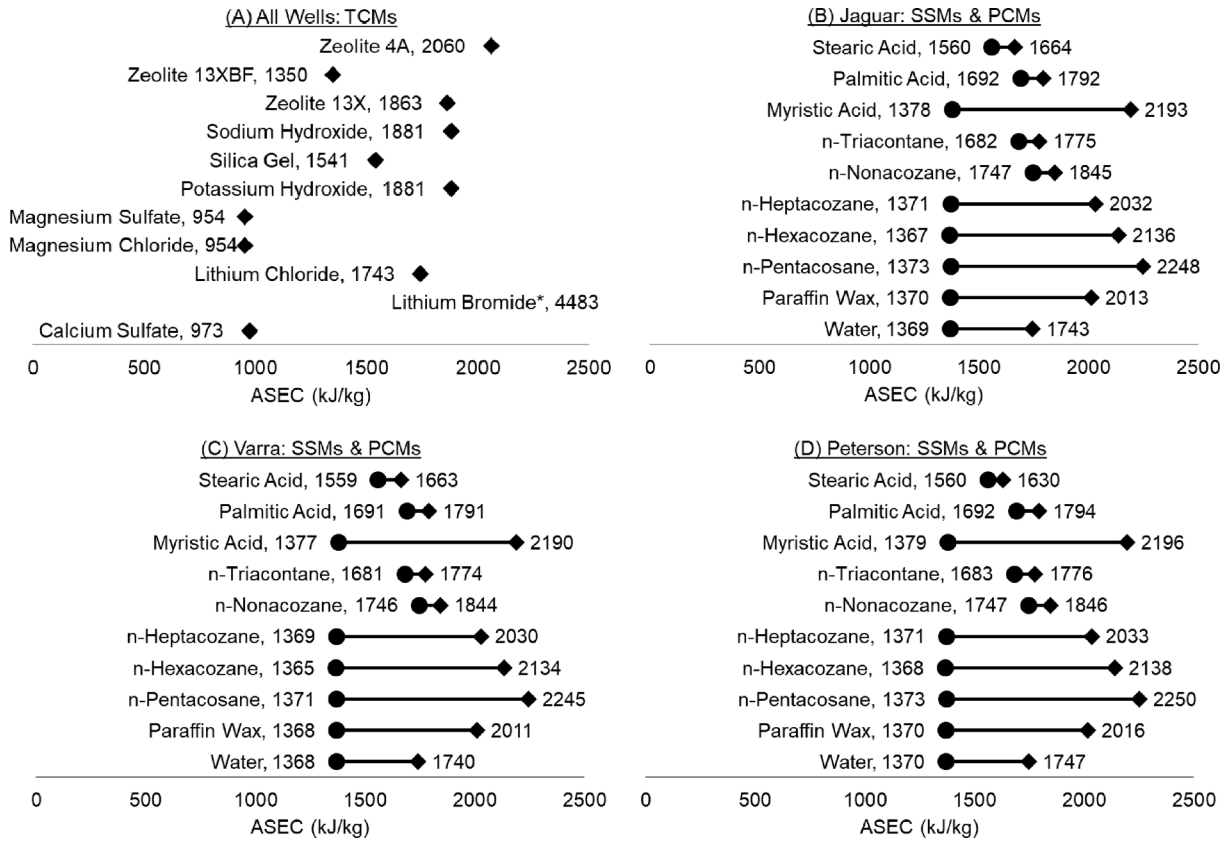

Fig. 7. Apparent specific energy consumption for storage materials at different wells. A) For thermo-chemical storage materials, performance is constant at all wells. Lithum Bromide, marked with an asterisk, has a discharge temperature lower than 60 °C and is not a viable option for waste heat storage when higher critical operating temperatures are used. Lithium Bromide also has an apparent specific energy consumption value of 4483 kJ/kg, which is beyond the scale of these plots. Sensible storage materials and phase change materials perform differently depending on wells and critical operating temperature. The average (B, Jaguar well), conservative (C, Varra well), and optimistic (D, Peterson well) scenarios are shown. The sensitivity of performance from change in critial operating temperature (40 to 60 °C) is represented with the bars. Lower apparent specific energy consumption (circles) is associated with a higher critical operating temperature. Higher apparent specific energy consumption is indicated by a diamond at the lower critical operating temperature. As the discharge temperature of TCMs does not change as heat is removed, the ASEC is only dependent on the material type but not the well or the operational condition of membrane distillation and therefore only have one apparent specific energy consumption value.

three materials increase to 0.29–0.71. In such scenarios, transporting waste heat, rather than FPW, could save up to 70% of transportation cost with the use of these appropriate TCMs for waste heat storage and transportation for decentralized FPW treatment. These results also indicate the importance of appropriately selecting thermal energy storage materials when storing waste heat to power on-site FPW treatment.

4. Conclusions

This study presents comprehensive analyses of waste heat collection, storage, and utilization for use in FPW treatment by membrane distillation with thermodynamic modeling. Our model was used to evaluate and compare three different scenarios: utilization of waste heat from hydraulic fracturing for on-site FPW treatment, utilization of waste heat from natural gas compressor stations for on-site FPW treatment, and utilization of waste heat from natural gas compressor stations for off-site FPW treatment. The first two scenarios require the storage of waste heat to overcome temporal and spatial disparities in waste heat availability and FPW treatment demand. The second scenario also requires the transportation of stored waste heat from natural gas compressor stations to the site of FPW production. The third scenario is used to compare the potential cost of FPW transportation to natural gas compressor stations with that of the second scenario. These three scenarios were considered for the treatment of FPW using membrane distillation for 20 wells in the Denver-Julesburg Basin and 21 waste heat storage materials.

Results showed that waste heat storage material selection is an important factor when leveraging waste heat for FPW treatment by membrane distillation, with the type of storage materials determining the utilization of waste heat and treatment capacity by membrane distillation. By tracking the change in temperature and energy content of the storage material throughout FPW treatment, we discovered that SSMs are disadvantageous compared to PCMs for waste heat storage due to the addition of latent heat storage in PCMs. Moreover, TCMs, which operate at constant temperatures, are capable of outperforming both SSMs and PCMs when TCMs with high (90 °C) discharge temperatures are used. Furthermore, the use of SSMs and PCMs limits the maximum waste heat utilization, a consequence of the critical temperature gap, which renders at least 11% and up to 83% of collected waste heat unusable by the membrane distillation treatment system.

This work, for the first time, quantifies the overall energy consumption of membrane distillation under continually changing conditions by calculating the apparent specific energy consumption. Comparing the minimum GOR (or critical SEC) of the wells to the attainable ASEC values for the proposed treatment systems, the average well could expect to see 100% FPW treatment when using calcium sulfate, magnesium chloride, or magnesium sulfate. These three TCMs enable the highest performance of MD and are the best options available for waste heat storage to be used in on-site FPW treatment. Furthermore, these three TCMs have transportation ratios between 0.29 and 0.97 for

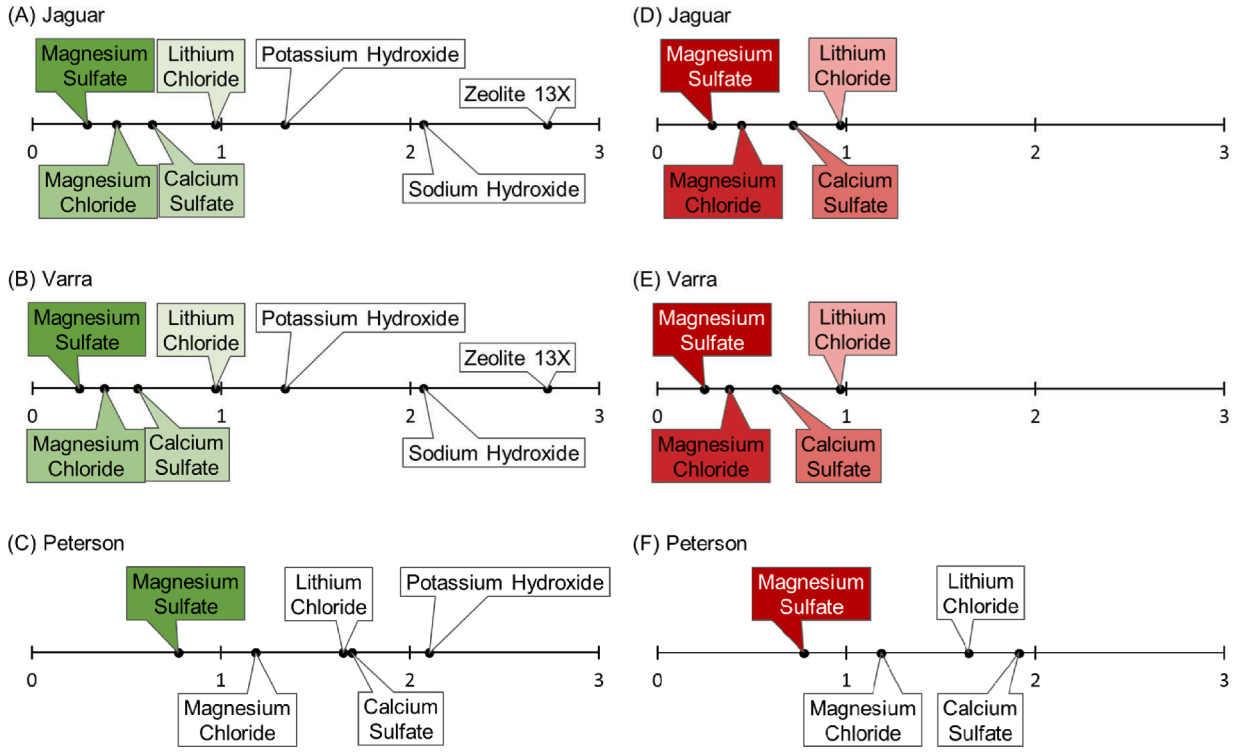

Fig. 8. Volumetric ratio (A-C, green) and transportation ratio (D-F, red) of waste heat storage material to raw flowback and produced water treated. For no wells would it be effiencent to transport waste heat from natural gas compressor stations using phase-change materials or sensible storage materials when compared to the transport of raw flowback and produced water to natural gas compressor stations for centralized treatment. At the Jaguar (A) and Varra (B) wells, four thermo-chemical materials (magnesium sulfate, magnersium chloride, calcium sulfate, and lithium bromide), highlighed in green (where a darker color of green denotes a material with better volumetric treatment capacity), require lower volumes of storage material than the volume of raw wastwater for transportation. At the Peterson (C) well, only magnesium sulfate is able to reduce the transprtation volume. With the added considertion of weight restrictions, the transportation ratio of materials at the Jaguar (D) and Varra (E) wells are not significanly affected, but the Peterson (F) well has no options for waste heat transportation. Materials with a ratio higher than 3 are not represented visually in the figure. Values for other wells are documented in the Supporting Information (Table S4-Table S23).

the average scenario of waste heat availability and FPW treatment demand, indicating that it is cost effective to transport the waste heat rather than the FPW when leveraging waste heat from natural gas compressor stations. In treatment scenarios which use these three TCMs as waste heat storage material, transporting waste heat rather than FPW could save up to 70% of transportation costs for FPW treatment.

Looking back at Figure 1, we see that both treatment scenarios for decentralized treatment are viable. Our results showed that decentralized treatment using stored waste heat from the hydraulic fracturing process (Fig. 1A) is viable in cases where sufficient waste heat generation is present. We also see that waste heat transportation (Fig. 1B) is an option for further consideration. When compared to wastewater transportation (Fig. 1C), waste heat transportation could decrease transportation costs by up to 70%. In both decentralized treatment scenarios, thermo-chemical storage materials are the best options for waste heat storage. The next steps in evaluating the feasibility of waste heat utilization for FPW treatment is to conduct a thorough economic analysis of the options for waste heat utilization and transportation throughout the Denver-Julesburg Basin, which includes system design and considerations such as system scale, and brine management.

CRediT authorship contribution statement

Brandi M. Grauberger: Conceptualization, Methodology, Software, Formal analysis, Data curation, Writing – original draft. **Garrett M. Cole:** Conceptualization, Writing – review & editing. **Cristian A. Robbins:** Conceptualization, Data curation, Writing – review & editing. **Jason C. Quinn:** Writing – review & editing, Supervision. **Tiezheng Tong:** Conceptualization, Writing – review & editing, Supervision. **Todd M. Bandhauer:** Conceptualization, Writing – review & editing, Supervision.

Declaration of Competing Interest

The authors declare the following financial interests/personal relationships which may be considered as potential competing interests: Brandi Grauberger reports financial support was provided by National Science Foundation.

Data availability

No data was used for the research described in the article.

Acknowledgement

This material is based upon work supported by the National Science Foundation under Grant No. 1828902. Any opinions, findings, and conclusions or recommendations expressed in this material are those of the authors and do not necessarily reflect the views of the National Science Foundation.

Appendix A. Supplementary data

Supplementary data to this article can be found online at https://doi.org/10.1016/j.apenergy.2022.120342.

References

[1] Barati R, Liang JT. A review of fracturing fluid systems used for hydraulic fracturing of oil and gas wells. J Appl Polym Sci 2014;131.
[2] Kondash AJ, Lauer NE, Vengosh A. The intensification of the water footprint of hydraulic fracturing. Science Advances. 2018;4:eaar5982.
[3] COGCC. Colorado Oil and Gas Information System. https://cogcc.state.co.us/data.html; 2021. [accessed 24 April 2021].
[4] Bell EA, Poynor TE, Newhart KB, Regnery J, Coday BD, Cath TY. Produced water treatment using forward osmosis membranes: Evaluation of extended-time performance and fouling. J Membr Sci 2017;525:77–88.
[5] Chang H, Li T, Liu B, Vidic RD, Elimelech M, Crittenden JC. Potential and implemented membrane-based technologies for the treatment and reuse of flowback and produced water from shale gas and oil plays: A review. Desalination 2019;455:34–57.
[6] Lester Y, Ferrer I, Thurman EM, Sitterley KA, Korak JA, Aiken G, et al. Characterization of hydraulic fracturing flowback water in Colorado: Implications for water treatment. Sci Total Environ 2015;512–513:637–44.
[7] Zhang Z, Du X, Carlson KH, Robbins CA, Tong T. Effective treatment of shale oil and gas produced water by membrane distillation coupled with precipitative softening and walnut shell filtration. Desalination 2019;454:82–90.
[8] Elimelech M, Phillip WA. The future of seawater desalination: energy, technology, and the environment. Science 2011;333:712–7.
[9] Esmaeilirad N, Carlson K, Omur OP. Influence of softening sequencing on electrocoagulation treatment of produced water. J Hazard Mater 2015;283:721–9.
[10] Kim S, Omur-Ozbek P, Dhanasekar A, Prior A, Carlson K. Temporal analysis of flowback and produced water composition from shale oil and gas operations: Impact of frac fluid characteristics. J Petrol Sci Eng 2016;147:202–10.
[11] McFarlane J, Bostick DT, Luo H. Characterization and modeling of produced water. Ground Water Protection Council Produced Water Conference, Colorado Springs, CO, Oct2002. p. 16-7.
[12] Rosenblum JS, Sitterley KA, Thurman EM, Ferrer I, Linden KG. Hydraulic fracturing wastewater treatment by coagulation-adsorption for removal of organic compounds and turbidity. J Environ Chem Eng 2016;4:1978–84.
[13] Lokare OR, Tavakkoli S, Rodriguez G, Khanna V, Vidic RD. Integrating membrane distillation with waste heat from natural gas compressor stations for produced water treatment in Pennsylvania. Desalination 2017;413:144–53.
[14] Robbins CA, Grauberger BM, Garland SD, Carlson KH, Lin S, Bandhauer TM, et al. On-site treatment capacity of membrane distillation powered by waste heat or natural gas for unconventional oil and gas wastewater in the Denver-Julesburg Basin. Environ Int 2020;145:106142.
[15] Tavakkoli S, Lokare OR, Vidic RD, Khanna V. A techno-economic assessment of membrane distillation for treatment of Marcellus shale produced water. Desalination 2017;416:24–34.
[16] Carrero-Parreño A, Onishi VC, Ruiz-Femenia R, Salcedo-Díaz R, Caballero JA, Reyes-Labarta JA. Optimization of multistage membrane distillation system for treating shale gas produced water. Desalination 2019;460:15–27.
[17] Lin S, Yip NY, Elimelech M. Direct contact membrane distillation with heat recovery: Thermodynamic insights from module scale modeling. J Membr Sci 2014;453:498–515.
[18] Schwantes R, Chavan K, Winter D, Felsmann C, Pfafferott J. Techno-economic comparison of membrane distillation and MVC in a zero liquid discharge application. Desalination 2018;428:50–68.
[19] Tavakkoli S, Lokare OR, Vidic RD, Khanna V. Systems-Level Analysis of Waste Heat Recovery Opportunities from Natural Gas Compressor Stations in the United States. ACS Sustainable Chem Eng 2016;4:3618–26.
[20] Hayes TD, Halldorson B, Horner PH, Ewing JJR, Werline JR, Severin BF. Mechanical Vapor Recompression for the Treatment of Shale-Gas Flowback Water. Oil and Gas Facilities. 2014;3:54–62.
[21] McGinnis RL, Hancock NT, Nowosielski-Slepowron MS, McGurgan GD. Pilot demonstration of the NH3/CO2 forward osmosis desalination process on high salinity brines. Desalination 2013;312:67–74.
[22] Christie KSS, Horseman T, Lin S. Energy efficiency of membrane distillation: Simplified analysis, heat recovery, and the use of waste-heat. Environ Int 2020;138:105588.
[23] Robbins CA, Carlson KH, Garland SD, Bandhauer TM, Grauberger BM, Tong T. Spatial analysis of membrane distillation powered by waste heat from natural gas compressor stations for unconventional oil and gas wastewater treatment in weld county, Colorado. ACS ES&T Eng 2021;1:192–203.
[24] Sonar D. Chapter 4 - Renewable energy based trigeneration systems—technologies, challenges and opportunities. In: Ren J, editor. Renewable-Energy-Driven Future: Academic Press; 2021. p. 125-68.
[25] Tatsidjodoung P, Le Pierrès N, Luo L. A review of potential materials for thermal energy storage in building applications. Renew Sustain Energy Rev 2013;18:327–49.
[26] ToolBox E. Water - Thermophysical Properties. https://www.engineeringtoolbox.com/water-thermal-properties-d_162.html; 2021. [accessed 1 June 2021].
[27] Murali G, Mayilsamy K, Arjunan TV. An Experimental Study of PCM-Incorporated Thermosyphon Solar Water Heating System. Int J Green Energy 2015;12:978–86.
[28] Chemeo. https://www.chemeo.com/; 2021. [accessed 1 June 2021].
[29] Abdul Hussain Ayash A. A New Correlation for Specific Heat of Normal Alkanes (C1-C30) as a Function of Temperature and Carbon Number. Journal of Engineering and Sustainable Development. 2019;23:166-74.
[30] NIST Chemisty WebBook. U.S. Secretary of Commerce National Institute of Standards and Technology; 2021.
[31] Kim S, Chen J, Cheng T, Gindulyte A, He J, He S, et al. PubChem in 2021: new data content and improved web interfaces. Nucleic Acids Res 2021;49:D1388–95.
[32] Jarimi H, Aydin D, Yanan Z, Ozankaya G, Chen X, Riffat S. Review on the recent progress of thermochemical materials and processes for solar thermal energy storage and industrial waste heat recovery. Int J Low-Carbon Technol 2019;14:44–69.
[33] Kalaiselvam S, Parameshwaran R. Chapter 6 - Thermochemical Energy Storage. In: Kalaiselvam S, Parameshwaran R, editors. Thermal Energy Storage Technologies for Sustainability. Boston: Academic Press; 2014. p. 127–44.
[34] Lizana J, Chacartegui R, Barrios-Padura Á, Valverde JM. Characterization of thermal energy storage materials for building applications. 3rd International Congress on Sustainable Construction and Eco-Efficient Solutions2017. p. 606-20.
[35] Kerskes H. Chapter 17 - Thermochemical Energy Storage. In: Letcher TM, editor. Storing Energy. Oxford: Elsevier; 2016. p. 345–72.
[36] Krönauer A, Lävemann E, Brückner S, Hauer A. Mobile Sorption Heat Storage in Industrial Waste Heat Recovery. Energy Procedia 2015;73:272–80.
[37] Yagi J, Akiyama T. Storage of thermal energy for effective use of waste heat from industries. J Mater Process Technol 1995;48:793–804.
[38] Yu N, Wang RZ, Wang LW. Sorption thermal storage for solar energy. Prog Energy Combust Sci 2013;39:489–514.
[39] Huang H, Li J, Huhetaoli OY, Wang C, Kobayashi N, et al. Porous-Resin-Supported Calcium Sulfate Materials for Thermal Energy Storage. Energy. Technology. 2016;4:1401–8.
[40] Ali A, Macedonio F, Drioli E, Aljlil S, Alharbi OA. Experimental and theoretical evaluation of temperature polarization phenomenon in direct contact membrane distillation. Chem Eng Res Des 2013;91:1966–77.
[41] Deshmukh A, Boo C, Karanikola V, Lin S, Straub AP, Tong T, et al. Membrane distillation at the water-energy nexus: limits, opportunities, and challenges. Energy Environ Sci 2018;11:1177–96.
[42] Lawson KW, Lloyd DR. Membrane distillation. J Membr Sci 1997;124:1–25.
[43] Khayet M, Matsuura T. Membrane distillation: principles and applications. 2011.
[44] Thiel GP, Tow EW, Banchik LD, Chung HW, Lienhard JH. Energy consumption in desalinating produced water from shale oil and gas extraction. Desalination 2015;366:94–112.
[45] Lokare OR, Tavakkoli S, Wadekar S, Khanna V, Vidic RD. Fouling in direct contact membrane distillation of produced water from unconventional gas extraction. J Membr Sci 2017;524:493–501.
[46] Bergman TL, Lavine AS. Fundamentals of Heat and Mass Transfer. 8th ed: John Wiley & Sons, Inc.; 2017.
[47] Patrick TT. Assuring Water Availability for Oil and Gas Operations. Water Resources IMPACT. 2015;17:11–3.